RSC Advances

ROYAL SOCIETY OF CHEMISTRY

www.rsc.org/advances

Preparation of Ni-Mo-P-PCTFE nanocomposite coating and evaluation of its Nano-tribological, Mechanical and electrochemical performance

S. Khameneh-asl[a], A. Farzaneh[a], S., H. Teymourinia[b], O. Mermer[c], M. G. Hosseini[* b]

a) Department of materials engineering, Faculty of Mechanical Engineering, University of Tabriz, Tabriz, Iran

b). Department of Physical Chemistry, Electrochemistry Research Laboratory, University of Tabriz, Tabriz, Iran

c) Department of Electrical and Electronic Engineering, Ege University, 35100, İzmir, Turkey

Abstract:

In this study, the tribological, mechanical and electrochemical performances of electrodeposited nickel-molybdenum-phosphorus (Ni-Mo-P) coating containing Polychlorotrifluoroethylene (PCTFE) nanoparticles were investigated. The nanocomposite coatings were deposited from potassium sodium tartrate containing electrolytes of in four different concentrations of PCTFE (0, 4, 8 and 20 g/l). The surface morphology, chemical and phase compositions of the Ni-Mo-P/PCTFE coatings were investigated using field-emission Scanning Electron Microscopy (FE-SEM), Energy Dispersive X-ray Analysis (EDAX) and X-ray Diffractrometry (XRD), respectively. Corrosion behaviour of the coatings was examined using potentiodynamic polarization and electrochemical impedance spectroscopy (EIS). Atomic force microscope (AFM) was used to investigate the tribological properties of the surface and in addition, their water-repellency were determined. The results show that there is a significant enhancement in corrosion resistance with the incorporation of PCTFE particles into the Ni-Mo-P matrix. It was also observed that the addition of PCTFE in the Ni-Mo-P alloy matrix has resulted in a smoother surface with a low friction coefficient and excellent water repellency.

Keywords: Ni-Mo-P/PCTFE nanocomposite coatings, electrochemical performance, Nano-tribological, Contact angle.

[*]Corresponding Author. Tel.: +984133393138; fax: +984133340191.
E-mail address: mg-hosseini@tabrizu.ac.ir .

1. Introduction:

Corrosion, wear, fatigue and rupture are amongst a wide range of failures that occur in coatings utilized in a variety of industrial applications and cause enormous losses to the national economy. Many research studies have been conducted to address this problem[1-5]. One approach is using composite coatings to improve the corrosion and wear resistances. Metal matrix composite coatings with ceramic and polymer reinforcement are used in industry[6-9].

There are a number of methods of depositing composite coatings such as electroless deposition[1], Electrophoretic deposition[10], cold[11] and thermal spray[12] and electrodeposition[13]. Amongst all these methods, electrodeposition is widely used in industrial applications because it is a well-established commercial technique for the production of thin films, metal coatings, as well as free-standing parts. Electrodeposition is a versatile technique as many different metals and alloys can be deposited onto a variety of conductive surfaces and they can provide composite and binary alloy coatings [13]. Metal matrix composites can be fabricated easily by electrodeposition and this approach enables micron- or submicron sizes of ceramic, metallic, or polymers particles to be co-deposited [14]. Significant research has gone into plating a series of composite coatings such as Ni-SiC[15], Ni-Al_2O_3[16], and Ni-Co-SiC[13], WS_2[17] which can effectively protect components from wear, corrosion and friction. Co-deposition of soft solid lubricants such as polytetrafluoroethylene (PTFE) and MoS_2 can increase the tribological resistance of the coating by reducing the friction coefficient[18, 19]. Moreover, composite coatings can improve other surface properties such as water repellency, self-lubrication and corrosion performance [20, 21].

Ni based alloys such as Ni – W – P or Ni – Mo – P have good mechanical and corrosion properties and are potential candidates as surface finishing and engineering materials[22- 24].

Recently, research studies have shown that self-lubricating composite coatings with binary and ternary alloy matrices can improve the protective properties of Ni based composite coatings[20, 22]. PCTFE is a hermoplastic chlorofluoropolymer and is similar to polytetrafluoroethene (PTFE), except that it is a homopolymer of the monomer chlorotrifluoroethylene (CTFE) instead of tetrafluoroethene. PCTFE has high tensile strength and low coefficient of thermal expansion. It has a good chemical resistance with zero-moisture absorption and non-wetting properties. PCTFE is resistant to the attack by most chemicals and oxidizing agents; a property which is exhibited due to the presence of high fluorine content. The results of our recent study indicated that PCTFE is a potential alternative for PTFE with improved properties [7]. In addition to the quality of the coating that was improved in our previous work, PCTFE can affect the corrosion and tribological behaviour of the coatings. To the best of our knowledge, there is no report on the corrosion and tribological behaviour of ternary Ni-Mo-P with PCTFE particles. Here, we want to develop new type of nano-composite coating with ternary alloy and self-lubricant particle to improve corrosion and nano-tribological performance of this type of coating.

In this research, Ni–Mo-P–PCTFE composite coatings were prepared on a copper substrate by electrodeposition in a Ni–Mo-P plating bath containing PCTFE particulates. The effects of PCTFE addition on the structural, surface morphology and corrosion behaviour of the coating were investigated.

2. Materials and method.

2.1. Preparation of composite coatings

In this study, a copper plate with a surface area of 1 cm^2 was used as the substrate. Before coating, the copper plate was subjected to a pre-treatment according to the following procedure. First, it was mechanically polished with different grades of emery papers up to #2000 and then

degreased in a 30% NaOH solution for 5 min, washed with distilled water, and dried in air. Then, the substrates were washed in distilled water and activated in 10% H_2SO_4 for 60 s at room temperature before the electrodeposition process.

Nickel composite electrodeposition was carried out using nickel sulfate ($NiSO_4 \cdot 6H_2O$) as a source of nickel, potassium sodium tartrate tetra hydrate ($C_4H_4KNaO_6 \times 4\ H_2O$) as the complexing agent, ammonium molybdate tetrahydrate ($(NH_4)8Mo_7O_{24}.4H_2O$) as the source of molybdenum and sodium hypophosphite($NaPO_2H_2$) as the source of phosphorous. Sodium dodecyl benzene sulfonate ($C_{18}H_{29}NaO_3S$, 99.99%) was employed as the surfactant to achieve better dispersion of second phase PCTFE particles (Aldrich, 0.02–0.2 μm). During electrodeposition, the electrolyte was agitated using a magnetic stirrer at 350 rpm; the pH and temperature of the plating baths were maintained at ±0.2 units and ±0.1 °C, respectively. The composition of the electrolyte and operating conditions are listed in Table 1. The coating thickness of all samples were about 10±1 μm.

Table 1.

Bath Composition		**Operating conditions**	
Nickel sulfate (g 1^{-1})	20	pH	7± 0. 5
Ammonium molybdate tetrahydrate (g 1^{-1})	5	Deposition temp. (°C)	45± 5
Potassium sodium tartrate (g 1^{-1})	85	Bath Vol. (ml)	200
sodium hypophosphite(g 1-1)	25	PTFE content (g 1^{-1})	0-20
Surfactant (g 1^{-1})	0.001	Voltage (V)	0.2
		Current density (mA/cm^2)	100

2.2 Characterization

X-ray diffraction (XRD) analysis (Bruker D2 Phaser, Cu Kα radiation) and Field Emission Scanning Electron Microscopy (FESEM, MIRA3 FEG-SEM Tescan) were utilized for structural

and morphological investigations, respectively. At the same time, the chemical compositions of the coatings were determined by energy dispersive spectroscopy (EDS). A KSV Attension Theta Lite Optical Tensiometer was used for water contact angle measurements. Deposit roughness, surface topography and friction were determined in air in the contact and noncontact mode Nanosurf Atomic Force Microscope (AFM). Coating thicknesses were measured by Hand-Held coating thickness measuring (instrument DELTASCOPE MP30E—Helmut Fischer, Germany) and verified by image analysis with optical microscope (Leica make, Model DMIRM, Olympus, Switzerland). Stability of the coating was controlled by The CROSS-HATCH TAPE test method according to the ASTM D3359.

Electrochemical studies were conducted at room temperature using 263A EG&G Princeton Applied Research (PAR) potentiostat/galvanostat and a standard three electrodes cell with a platinum electrode as counter electrode, saturated calomel electrode (SCE) as reference electrode and samples with an exposed area of 1 cm^2 as working electrode in an aqueous solution of 3.5 wt. % NaCl. The potentiodynamic polarization curves and open-circuit potential (EOCP) were recorded using a constant voltage scan rate of 1 mVs^{-1}. Electrochemical impedance spectroscopy (EIS) experiments were done in the frequency range of 100 KHz-10 MHz and the perturbation amplitude was ± 5 mV.

3. Results and discussion:

3.1 characterization of the coating

SEM micrographs of the surface of coatings electrodeposited from the solutions containing 0 and 20 gl^{-1} PCTFE are shown in Fig.1. It can be seen that the PCTFE particles decreased the nodules

size of the Ni-Mo-P coating and improved the homogeneity of the surface. The Ni-Mo-P-PCTFE coating depicts a smooth and compact surface, which is consistent with our previous work[7].

The chemical compositions of the coatings were determined by EDS and the results are shown in Fig.1 whilst their weight percentages are listed in Table 2. According to these results the Ni-Mo-P coating, is mainly composed of 59.48 wt. % Ni, 13.94 wt.% Mo and 26.58 wt. %. of P. By addition of PCTFE to the coating bath, the concentration of Mo decreased and that of P increased. According to the chemical formula of PCTFE, there is F and Cl in the PCTFE composition and they can be the pointer of PCTFE material. The fact that F and Cl have been detected in the coating is a good indication that PCTFE nanoparticles was combined into the Ni-Mo-P coatings successfully.

Table 2.

	Ni (%wt)	Mo (%wt)	F (%wt)	C (%wt)	P (%wt)	Cl (%wt)
Ni-Mo-P	59.48	13.94	-	-	26.58	-
Ni-Mo-P-PCTFE (20g l^{-1})	52.83	5.43	3.56	10.33	27.40	0.45

Fig. 2 illustrated the XRD results of samples produced using different plating conditions. The XRD patterns indicate the main peaks corresponding to (111), (200) crystallographic planes of nickel at 2θ = 43.92° and 51.03°. The Ni-Mo intermetallic compound peak appears around 2θ=74.5 whilst the Ni-Mo phase appears at the same Ni (200) plane. when PCTFE particles are added to the electrolyte, a new amorphous shape pattern appeared which expresses the presence of a PCTFE phase in the deposition and intensity change and broadening of the reflection from Ni (1 1 1) plane happened. By increasing the PCTFE concentration this trend can be seen more

effectively and the crystallinity of the coating when 20 gl^{-1} PCTFE is added is lower than for the other coatings. In general, Ni-Mo-P-PCTFE deposits have mixed crystalline and amorphous microstructures. Fig. 3 shows the effects of PCTFE concentration on the structure of the Ni-Mo-P-PCTFE coating. This indicates that the peaks became shorter and wider with addition of PCTFE particles. The full width of the peaks at their half maximum (FWHM) also decreased with PCTFE concentration. These changes signify that PCTFE reduced the crystalline size of coatings[1] as estimated by using the Scherrer formula [2, 26]:

$$D = 0.9\lambda / \beta\cos\theta \quad (1)$$

Where D, λ, β and θ are grain size, wavelength, peak width and diffraction angle, respectively. This equation shows that broadening of peaks (β) is inversely proportional to the grain size (D)[25]. Fig. 4 shows the average crystalline size of prepared samples with regard to the PCTFE concentrations. Results show that adding PCTFE decreases crystal size in prepared coatings.

For more quantification of the different crystal planes, the 'Relative Texture Coefficient' (RTC) of the coating were also calculated. This method can be used for quantify crystal planes in electrodeposited metal-based coatings[26]. The Relative Texture Coefficient or RTC for a (hkl) crystal plane is defined as:

$$RTC_{(hkl)} = 100 \times \frac{I_{(hkl)} / I^{\circ}_{(hkl)}}{\sum_{1}^{2} I_{(hkl)} / I^{\circ}_{(hkl)}} \quad (2)$$

where $I_{(hkl)}$ are the relative intensities of the (hkl) refection, $I^{0}_{(hkl)}$ is the intensity of the reflection for the same crystal plane in a standard Ni powder sample. For this purpose the two basic lines of the total reflection lines are considered (111) and (200). Fig. 5 illustrated $RTC_{(hkl)}$ values for

all the Ni crystal planes in each 2θ scan. As it shown, the RTC $_{(111)}$ decreased by increasing PCTFE concentration and RTC $_{(200)}$ is increased. The changings in RTC value can be signified the value of the relative texture coefficient of each crystalline orientation[27].

The Aruna *et al.*[27] claimed that "the composite particle can be attributed to the changes taking place in the nature of adsorption desorption phenomena in the region of the catholyte area when surface charged oxides arrive at the cathode and are loosely adsorbed or partially submerged onto the growing nickel grains". The same trend occurs in our results and PCTFE changed the surface crystal orientation. The RTC $_{(111)}$ prolapsed from 30 to 12 in presence of PCTFE. The RTC variance can be attributed to changing surface morphology in nano composite coating[28].

3.2 Tribology and mechanical performance

Atomic force microscope (AFM) in two noncontact and contact modes was used to study the surface topography and lubricating properties of the prepared coatings[28]. The 3D AFM morphological images of the coatings are shown in Fig. 6. Combined with the R_a roughness factor results in Fig. 7. , it is obvious that the Ni-Mo-P coating is much rougher than PCTFE composite coatings, which confirms the XRD and SEM results. The incorporation of PCTFE particles increases the crystal growth site and reduces the grain size and hence improves the surface homogeneity. It should also be noted that in the Ni-Mo-P coating the micro-cracks have been observed as it can be seen in the 3D AFM image.

The friction map has been measured by using the AFM in contact mode and measuring the torsional deflection of the cantilever. The objective of this part of the study was to investigate the effect of surface morphology on the tribology of the coating. Fig. 8 gives the friction results, and

it can be seen that the tribological behaviour of the coating depends on PCTFE concentration. In Ni-Mo-P sample, the friction force fluctuated in a range of -0.06-0.05 V. However, as the PCTTFE concentration increased, this fluctuation decreases to the range of -0.02-0.02 V. In addition, the nano-composite coatings showed a smooth flat friction behaviour and better tribological properties compared with the Ni-Mo-P sample whist the coatings produced with 20g l^{-1} of PCTFE added to the electrolyte exhibited the best friction behaviour with low force and smooth behaviour. The low friction force was anticipated due to the self-lubricating properties of the PCTFE nano-composite coating.

Fig. 9 depicts the nano-indentation results of the coatings with different concentrations of PCTFE particles. The Y axis is force and X axis is indentation depth. It is apparent that by raising the PCTFE concentration, the indentation depth increased. Indeed, it can be stated that, by increasing the PCTFE concentration in the electrolyte, the elastic behaviour of coating increased because of the reduced hardness. However the coating deposited in the presence of 20 $g1^{-1}$ PCTFE showed a slightly different trend in indentation results. The coatings produced under these conditions exhibited higher elastic load than the other samples and these results can be explained by reference to the XRD results i.e. the coating produced with an addition of 20 g l^{-1} PCTFE showed the lowest grain or crystalline size which may have caused an increase in the elastic force.

Stability and adhesion of the coating was evaluated by CROSS-HATCH methods. Results show that the coatings have good adhesion and all the samples pass the grade 5B level according to the ASTM D3359 standard.

3.3 Corrosion properties

The variation of the open circuit potential (OCP) of the the Ni-Mo-P and Ni-Mo-P-PCTFE depositions in 3.5% NaCl electrolyte are shown in Fig.10. Above 4 gl^{-1}, the addition of PCTFE particles to the plating solution produced coatings with more positive OCP i.e. the nano-composite coatings with PCTFE particles are more noble than the Ni-Mo-P coatings. From these results it can be stated that the reinforcement of PCTFE particles into the coatings generally improves the corrosion resistance whilst the coating produced with a PCTFE concentration of 20 gl^{-1} exhibited the highest value of the OCP.

The potentiodynamic polarization plots of the Ni-Mo-P-PCTFE coatings are illustrated in Fig. 11. It is clear that the addition of PCTFE particles, regardless of the concentration used, shifted the polarization plots of the Ni-MO-P-PCTFE coating to positive potentials and low current densities. The corrosion current density of the coatings was calculated by using Tafel extrapolation and these, along with the OCP values are listed in Table 3. The results indicate that by increasing the PCTFE concentration, the Ni-Mo-P-PCTFE coatings corrosion rate is reduced. This reveals that the PCTFE affects the electrochemical behaviour of the Ni-Mo-P coating and improved its corrosion performance. The coating produced by adding 20g/l PCTFE to the deposition solution showed the lowest corrosion current density and highest polarization resistance compared to the other coatings.

Table. 3.

System studied	E_{corr} (mV vs. SCE)	i_{corr} (µA cm^{-2})
Ni-Mo-P	-149.09	10
Ni- Mo-P-PCTFE (4 g l^{-1})	-120.87	8
Ni- Mo-P-PCTFE (8 g l^{-1})	65.37	2.8
Ni- Mo-P-PCTFE (20 g l^{-1})	83.59	0.1

The Nyquist and bode plots of the Ni-Mo-P-PCTFE coating as a function of PCTFE concentration are shown in Fig. 12 and 13 respectively. The Nyquist plots of all depositions have shown a semicircular arc with two capacitive loops that twisted in each other. These two loops, suggest the existence of one surface layer on the coating surface and one charge transfer layer in the coating and substrate interface. In these graphs two time constants (τ = R.C) are observed. The time constant in high frequency and low frequency are related to the coating and double layer respectively. The experimental and calculated impedance results of Ni-Mo-P-PCTFE 20g l^{-1} are presented in Fig. 14, which shows a good agreement between experimental and simulated data. The equivalent circuit has been simulated by Z'view(II) software and the parameters derived from EIS are summarized in Table 4.

Table 4.

Element	PCTFE (0g 1^{-1})	PCTFE (4 g 1^{-1})	PCTFE (8 g 1^{-1})	PCTFE (20 g 1^{-1})
R_s (Ω cm^2)	8.46	7.12	6.77	7.89
CPE_1-T(F. cm^{-2})	0.00030	0.00024	0.00009	0.00007
CPE_1-P	0.8827	0.8566	0.8916	0.9819
R_2 (Ω cm^2)	1995	2300	2500	13325
CPE_2-T(F. cm^{-2})	0.004024	0.000343	0.000059	0.000156
CPE_2-P	0.4615	0.2002	0.2659	0.4636
R_3 (Ω cm^2)	2443	4047	9745	29927
Error (%)	0.001	0.02	0.003	0.004

According to this table, Rs is the solution resistance, R_2 and CPE_1 are respectively the resistant and constant phase element related to the coating, R_3 and CPE_2 are resistant and constant phase element of coating and substrate interface. The high charge transfer resistance is indicative of high corrosion resistance. The results of the EIS indicated a similar trend in the corrosion

resistance to that seen in the potentiodynamic polarization studies. The highest Rct value was obtained for the Ni-Mo-P-PCTFE nanocomposite coating produced when 20 gl^{-1} of PCTFE particles were added to the electrolyte. These electrochemical studies have revealed that the incorporation of PCTFE particles into the Ni-Mo-P coating improved its corrosion resistance. This improvement can be explained in a number of ways. Firstly, addition of PCTFE is likely to reduce the effective metallic surface area of the Ni-Mo-P-PCTFE coatings compared to that of the Ni-Mo-P coating. By calculating the volume fraction of the PCTFE particles in the coatings, (using the density and concentration in EDS results[1]), it can be proposed that the surface area covered with PCFTE particles on the surface of the coatings is the same as their vol. %. Taking this approach, the ratio of the metallic surface area of the Ni-Mo-P-PCTFE coatings to that of the Ni-Mo-P coating may be less than 68% [1]. The EDS results from this study showed that as more PCTFE was added to the electrolyte the lower was the Mo content in the coatings. Régis L. Melo et. al. [29] reported that the presence of high concentrations of Mo in Ni-Mo-P coatings caused the deposit to be cracked, which obviously compromised the corrosion-resistance and hardness properties of the Ni–Mo coatings. Also Z .Abdel Hamid, et.al[30], are investigated the influence of electrodeposition parameters on the characteristics of Ni-Mo-P film. Taking these findings into consideration the coatings with low Mo would be expected to have better corrosion resistance. In addition, S. Sangeetha et al.[20] reported the effect of PTFE on the corrosion performance of Ni-W-PTFE coatings. They claim that the addition of the polymer material filled the cracks and holes of the alloy matrix and hence the self-lubricating PTFE polymer layer enhanced the anticorrosion property of the nano-composite coatings. The results obtained in this study are therefore in good agreement with the literature. The SEM and AFM images of the Ni-Mo-P-PCTFE coatings exhibit a uniform and nonporous structure and the XRD results suggest a small

crystalline size. These properties may enhance the compactness of the deposit and limit diffusion of the corrosive ions into the deposition which in turn will lead to the better corrosion performance as determined by the electrochemical analysis. The previous reports of our group[7] showed that a further increase in the PCTFE concentration (above 8 gl^{-1}) in the electrolyte causes a decrease in the corrosion resistance of coatings. However with the ternary alloy deposited in this study the opposite result has been observed. This can be explained by effect of Mo contribution by PCTFE. The Ni-Mo-P-PCTE coating with 20 g 1^{-1} PCTFE nanoparticles exhibited the lowest corrosion rate with highest charge transfer resistant among the composite coatings with the inhibition efficiency by approximately 96%.

The comparison of the previous works with this research is tabulated in table 5 . Table 5 is demonstrated the corrosion results of as-plated nickel alloy coatings in 3.5% sodium chloride solution by potentiodynamic polarization technique. It can be observed that a significant decreasing corrosion rate of Ni-Mo-P-PCTFE coatings (20 g/L) respect to others work are shown in table5 ($i_{corr}(0.1\mu A/cm^2)$)

Table 5. Corrosion characteristics of as-plated nickel alloy coatings in 3.5% sodium chloride solution by potentiodynamic polarization technique

Ni alloy nanocomposites	-Ecorr (mV vs. SCE)	icorr($\mu A/cm^2$)
Ni–P	342	0.456
Ni–W–P	389	0.685
Ni–W–Cu–P [31]	305	0.481
Ni–P	350	0.80
Ni–Cu–P	330	0.92
Ni–W–P	385	0.76
Ni–W–Cu–P [32]	330	0.72
Ni– W– P– WS_2 [33]	380	0.729
Co–27%Ni	545	2.0
Co–38%Ni	470	2.1
Co–12%Ni–13%Mo [34]	636	1.5
Ni-Co-SiC20 [13]	225	0.190

Ni-Mo [35]	530	3.31
Ni–Mo–MMT [36]	400	0.13-0.51
Ni–Mo5.7%–P [30]	295	3.2
Ni-Mo-P-PCTFE (20 g/L) This work	83.59	0.1

3.4 Water contact angle measurements

The contact angle measurement was measured to understand the water-repellency behaviour of the nano-composite coatings. Contact angle theory is the state of location of one droplet on the homogeneous flat solid surface. The surface wettability depends on surface chemical composition and surface roughness. The contact angle is correlated by three interfacial free energies: free energies at the solid-air (γ_{SV}), solid-liquid (γ_{SL}) and liquid-air (γ_{LV}) interfaces, by the Young's equation [3]:

$$\cos\theta_{flat} = \frac{\gamma_{SV} - \gamma_{SL}}{\gamma_{LV}} \quad (3)$$

As it is shown in Eqn. (1), by decreasing the surface free energy of the solid-air interface (γ_{SV}) the surface hydrophobicity will be increased. When θ_{flat} is smaller than 90°, the solid surface is considered hydrophilic; when θ_{flat} is greater than 90°, the solid surface is called hydrophobic. The volume of the water droplet was 1 µL which was dispensed onto the nano-composite coatings produced in this study and the findings are shown in Fig. 15. It is known that PCTFE is a low surface energy polymer and by increasing the concentration of the PCTFE in the coating the surface energy is decreased and as a result the water contact angle is increased. The results show the self-lubricating PCTFE polymer has improved the water repellency from 82^0 to 102^0 when a high concentration of PCTFE is used in the electrolyte. This may also be a further reason why the corrosion properties of the coating are enhanced by incorporation of PCTFE i.e. water is repelled from the surface and therefore corrosion is less likely.

4. Conclusion:

In this paper, the structure, morphology, tribology, mechanical and corrosion performance of the electrodeposited Ni-Mo-P-matrix composite coatings co-deposited with PCTFE particles were evaluated. Co-deposition of the PCTFE particles into the Ni-Mo-P coating changed the structure and morphology of the deposited coating and decreased the nodules and crystalline size and also porosity. Increase in the PCTFE concentration of coating bath, the elastic behaviour of coating increased. The coatings produced with a concentration of 20 g 1^{-1} PCTFE in the electrolyte showed the lowest friction force in comparison with other samples. The corrosion performance and water repellency of the Ni-Mo-P coating was improved by co-deposition of the PCTFE particles.

Acknowledgements

The authors would like to acknowledge the financial support of the Office in Charge of Research of Iranian Nanotechnology Society and the financial support of the Office of Vice chancellor in charge of research of University of Tabriz.

Reference:

.1 A. Farzaneh, M. Mohammadi, M. Ehteshamzadeh and F. Mohammadi, *Applied Surface Science*, 2013, **276**, 697-704.
.2 A. Farzaneh, M. Ehteshamzadeh and M. Mohammadi, *Journal of Applied Electrochemistry*, 2011, **41**, 19-27.
.3 A. Farzaneh, Z. Ahmad, M. Can, S. Okur, O. Mermer and A. K. Havare, 2015.
.4 Amir Farzaneh, Maysam Mohammdi, Z. Ahmad and I. Ahmad, *Aluminium Alloys - New Trends in Fabrication and Applications*, 2012, **InTech**. ,
.5 A. F. a. B. J. A. A. Zaki Ahmad, in *Recent Trends in Processing and Degradation of Aluminium Alloys*, ed. Z. Ahmad, InTech, 1 edn., 2011, DOI: DOI: 10.5772/23631, ch. 16.

.6 M. Hosseini, M. Abdolmaleki and J. Ghahremani, *Corrosion Engineering, Science and Technology*, 2014, **49**, 247-253.
.7 M. Hosseini, M. Abdolmaleki, S. Ashrafpoor and R. Najjar, *Surface and Coatings Technology*, 2012, **206**, 4546-4552.
.8 M. Hosseini, M. Abdolmaleki, S. Seyed Sadjadi, M. Raghibi Boroujeni, M. Arshadi and H. Khoshvaght, *Surface Engineering*, 2009, **25**, 382-388.
.9 I. Tudela, Y. Zhang, M. Pal, I. Kerr and A. J. Cobley, *Surface and Coatings Technology*, 2014, **259**, 363-373.
.10 J. Cho, S. Schaab, J. A. Roether and A. R. Boccaccini, *Journal of Nanoparticle Research*, 2008, **10**, 99-105.
.11 S. R. Bakshi, V. Singh, K. Balani, D. G. McCartney, S. Seal and A. Agarwal, *Surface and Coatings Technology*, 2008, **202**, 5162-5169.
.12 X. Zheng, M. Huang and C. Ding, *Biomaterials*, 2000, **21**, 841-849.
.13 B. Bakhit, A. Akbari, F. Nasirpouri and M. G. Hosseini, *Applied Surface Science*, 2014, **307**, 351-359.
.14 Y. H. Ahmad and A .M. Mohamed, *International Journal of Electrochemical Sciences*, 2014, **9**, 1942-1963.
.15 M. Vaezi, S. Sadrnezhaad and L. Nikzad, *Colloids and Surfaces A: Physicochemical and Engineering Aspects*, 2008, **315**, 176-182.
.16 R. Oberle, M. Scanlon, R. Cammarata and P. Searson, *Applied physics letters*, 1995, **66**, 19-21.
.17 I. Tudela, Y. Zhang, M. Pal, I. Kerr and A. J. Cobley, *Surface and Coatings Technology*, 2015, **276**, 89-105.
.18 M. Mohammadi and M. Ghorbani, *Journal of coatings technology and research*, 2011, **8** , .533-527
.19 M. Mohammadi, M. Ghorbani and A. Azizi, *Journal of coatings technology and research*, 2010, **7**, 697-702.
.20 S. Sangeetha, G. P. Kalaignan and J. T. Anthuvan, *Applied Surface Science*, 2015, **359**, 412-419.
.21 Y.-H. You, C.-D. Gu, X.-L. Wang and J.-P. Tu, *Int. J. Electrochem. Sci*, 2012, **7**, 12440-12455.
.22 Z. Guo, X. Zhu and R. Xu, *Materials science and technology*, 2004, **20**, 257-260.
.23 M. Hosseini, H. Teymourinia, A. Farzaneh and S. Khameneh-asl, *Surface and Coatings Technology*, 2016.
24. A. Farzaneh, M. G. Hosseini, S. K. Asl and O. Mermer., *Int. J. Electrochem. Sci,* 2016. **11**: p. 5140-5153.
25 A. Farzaneh, M. Ehteshamzadeh, M. Ghorbani and J. V. Mehrabani, *Journal of coatings technology and research*, 2010, **7**, 547-555.
26 I. Tudela, Y. Zhang, M. Pal, I. Kerr, T. J. Mason and A. J. Cobley, *Surface and Coatings Technology*, 2015, **264**, 49-59.
27 S. Aruna, P. Lashmi and H. Seema, *RSC Advances*, 2016.
28. G. Xie, J. Ding, B. Zheng and W. Xue, *Tribology International*, 2009, **42**, 183-189.
29. R. L. Melo, P. N. Casciano, A. N. Correia and P. d. Lima-Neto, *Journal of the Brazilian Chemical Society*, 2012, **23**, 32.334-8

30. Z .Abdel Hamid, H. Hassan, *Surface and Coatings Technology*, 212 (2012) 37-45.

31. J. Balaraju, V. E. Selvi, V. W. Grips and K. Rajam, *Electrochimica acta*, 2006. **52**(3): p. 1064-1074.

32. J. Balaraju, and K. Rajam, *Surface and coatings technology,* 2005. **195**(2): p. 154-161.
33. S. Ranganatha, T. Venkatesha, and K. Vathsala, *Industrial & Engineering Chemistry Research,* 2012. **51**(23): p. 7932-7940.
34. E. Gómez, E. Pellicer, and E. Vallés, *Electrochemistry communications,* 2005. **7**(3): p. 275-281.
35. P.-C.Huang, K.-H. Hou, G.-L. Wang, M.-L. Chen and J.-R. Wang., *Int. J. Electrochem. Sci,* 2015. **10**(6): p. 4972-4984.
36 Y. H.Ahmad, J. Tientong, M. Nar, N. D'Souza, A. Mohamed and T. D. Golden., *Surface and Coatings Technology,* 2014. **259**: p. 517-525.

Table captions:

Table 1. Electrodeposition bath composition and operating conditions

Table 2. EDS chemical composition analysis results for various Ni-Mo-P-PCTFE coatings.

Table. 3. Values of Ecorr and icorr of Ni-Mo-P-PCTFE composite coatings in 3.5 wt. % NaCl solution.

Table 4. Fitting results of the impedance spectra of Ni-Mo-P-PCTFE composite coatings in 3.5 wt. % NaCl solution.

Table 5. Corrosion characteristics of as-plated nickel alloy coatings in 3.5% sodium chloride solution by potentiodynamic polarization technique

Figure captions:

Fig. 1: SEM micrographs of the surface of a) Ni–Mo-P and b) Ni-Mo-P-PCTFE 20g 1^{-1} coatings and EDS images and elemental composition of c) Ni–Mo-P and d) Ni-Mo-P-PCTFE 20g 1^{-1} coatings.

Fig. 2. X ray Diffractograms of the a) Ni–Mo-P b) Ni-Mo-P-PCTFE 4 $g1^{-1}$ c) 8 g 1^{-1} and d) 20 gl^{-1} coatings.

Fig.3: X-ray Diffractograms of the a) Ni–Mo-P and Ni-Mo-P-PCTFE 4 $g1^{-1}$ b) 4 g 1^{-1} and 20 gl^{-1} coatings in high magnification.

Fig.4: Crystalline size of prepared samples as a function of PCTFE concentration.

Fig.5 RTC (hkl) results for different crystal planes observed in prepared samples as a function of PCTFE concentration.

Fig. 6. AFM morphological images of a) Ni–Mo-P b) Ni-Mo-P-PCTFE 4 g 1^{-1} c) 8 g 1^{-1} and d) 20 g 1^{-1} coatings.

Fig.7: Ra roughness factor of prepared samples as a function of PCTFE concentration.

Fig.8 AFM Friction force data of prepared samples as a function of PCTFE concentration.

Fig. 9. AFM Load -displacement graphs for very low loads and indentation depths of prepared samples.

Fig.10. Open-circuit potential vs. time curves in 3.5% NaCl solution of pure Ni-Mo-P and Ni-Mo-P-PCTFE coatings.

Fig. 11. Polarization curves of Ni-Mo-P and Ni-Mo-P-PCTFE composite coatings in 3.5 wt. % NaCl solutions at scan rate of 0.2 mV s^{-1}.

Fig. 12. Equivalent circuit and Nyquist plots of Ni-Mo-P and Ni-Mo-P-PCTFE composite coatings in 3.5 wt. % NaCl solution.

Fig. 13. Bode-Phase plots for Ni-Mo-P and Ni-Mo-P-PCTFE composite coatings in 3.5 wt. % NaCl solution.

Fig. 14: Experimental and modeled Nyquest and bode spectrum of the Ni-Mo-P-PCTFE 20gl^{-1} coating.

Fig.15. Contact angle measurements of a water droplet (1 μL) on the Ni-Mo-P-PCTFE Nano composite coatings.

Fig.1

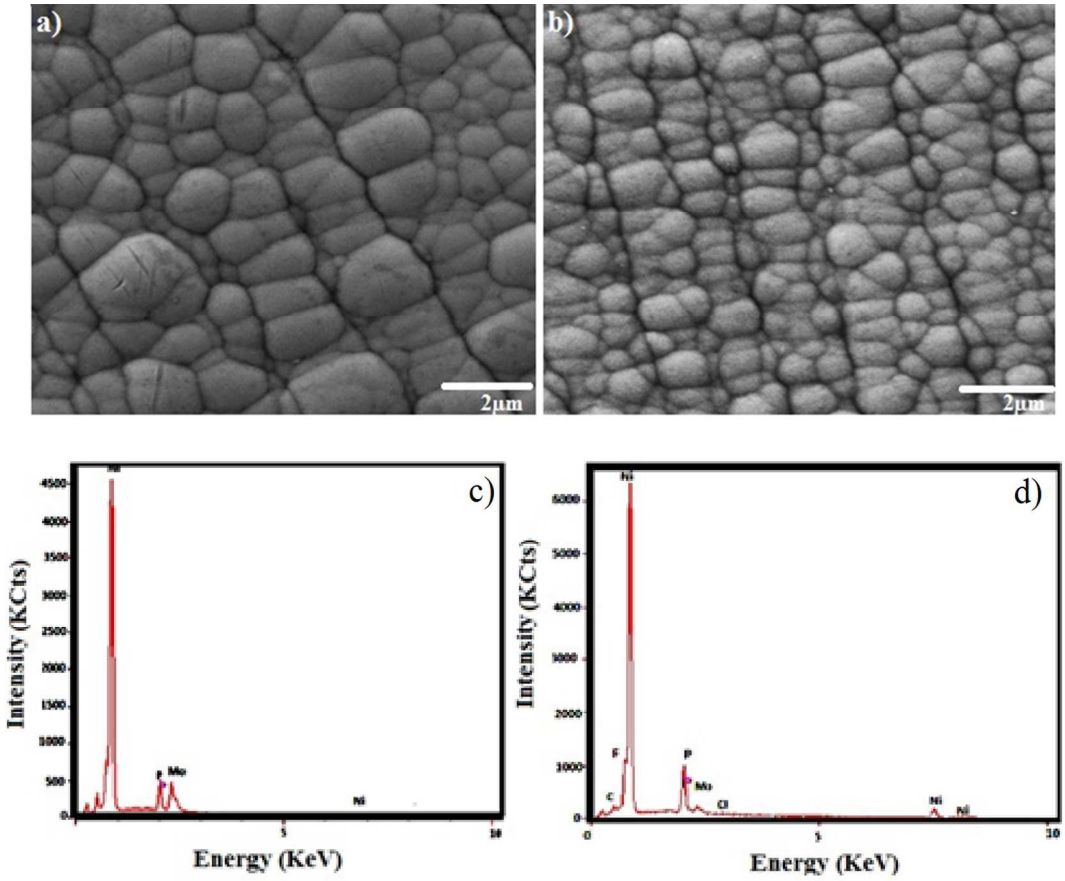

Fig.2

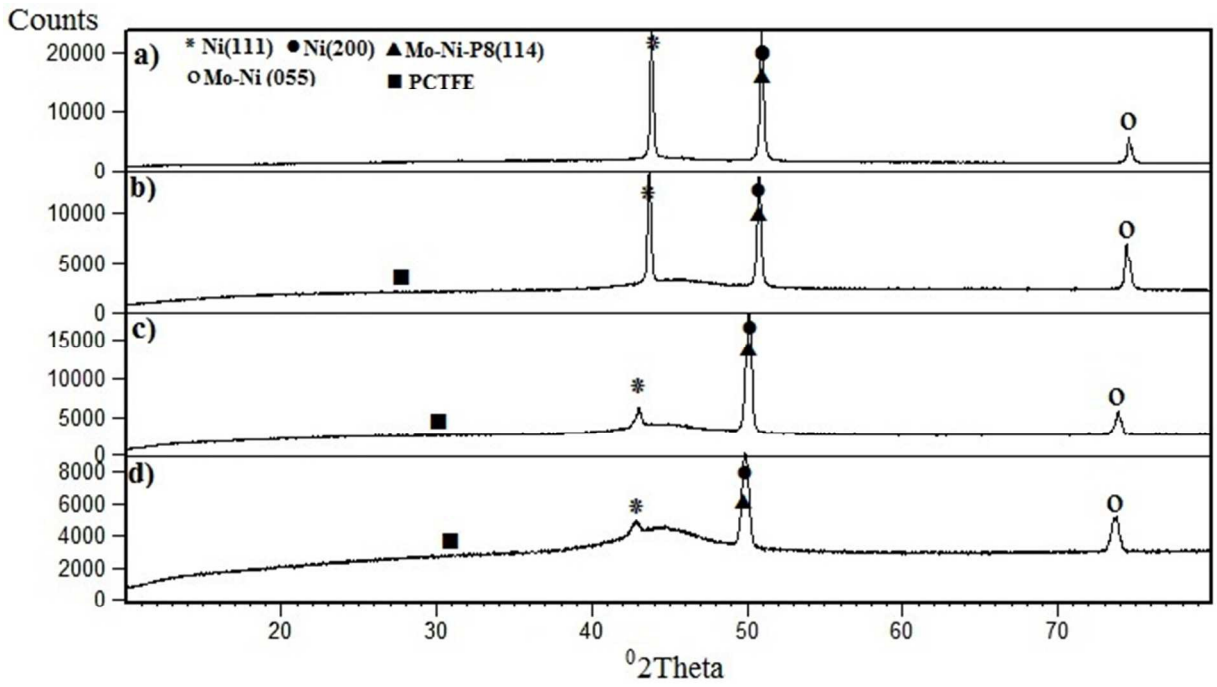

Fig.3

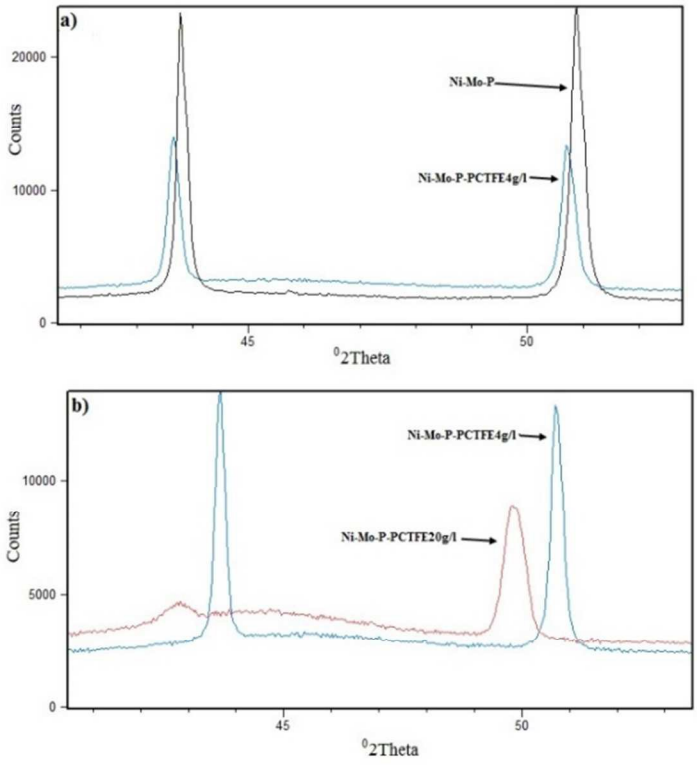

Fig.4

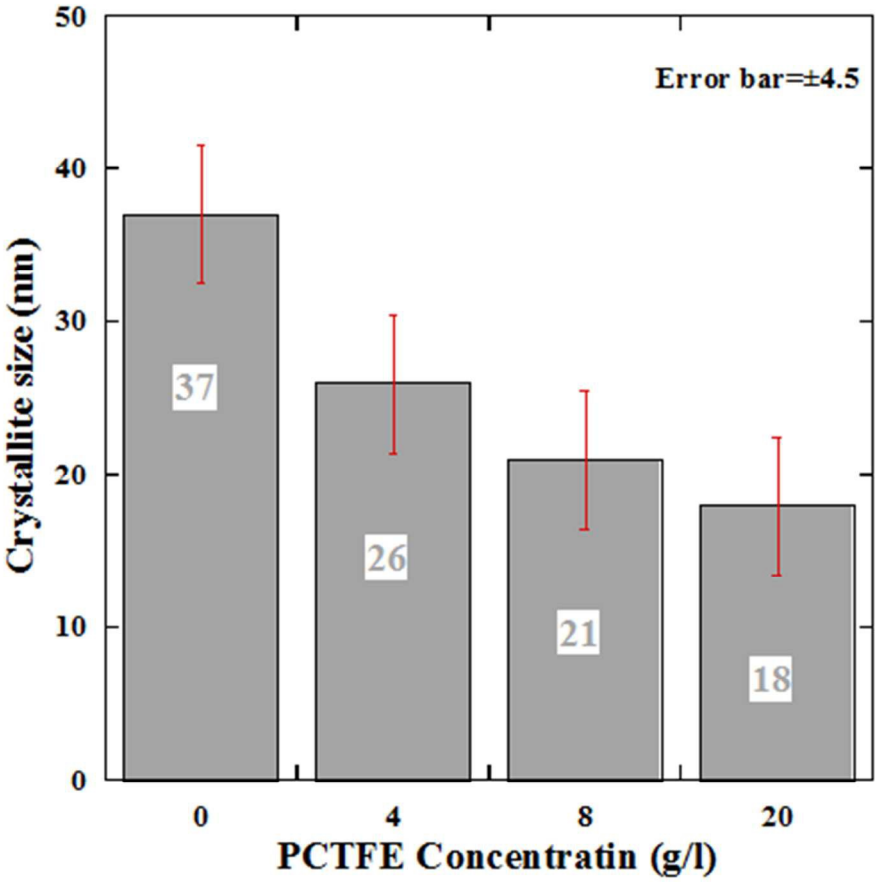

Fig.5

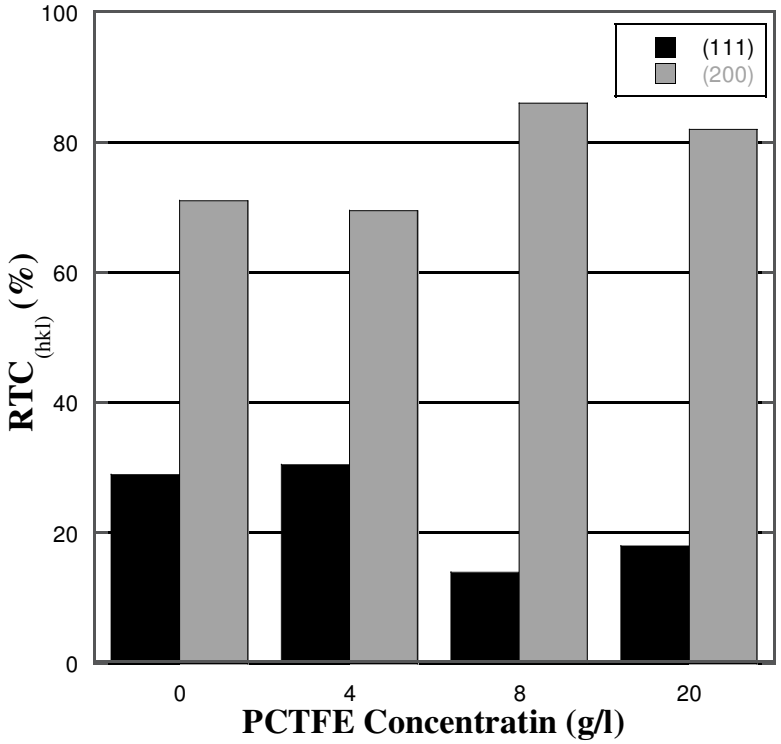

Fig.6

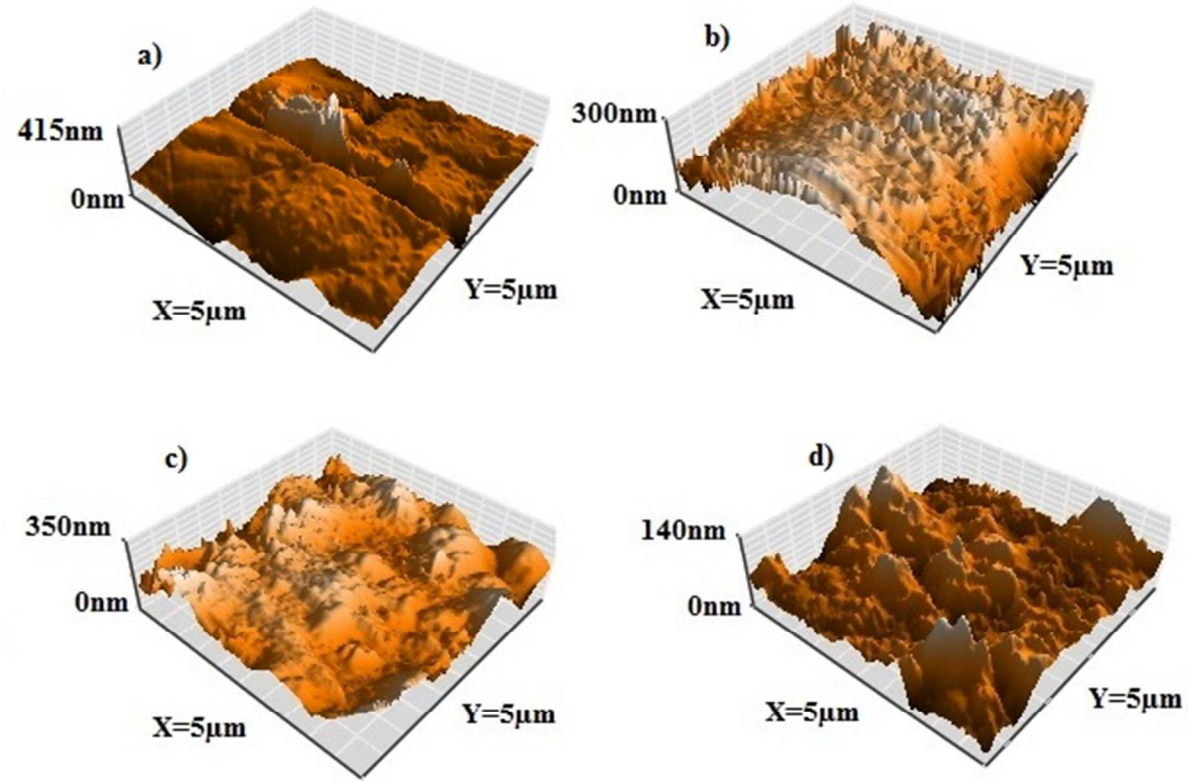

Fig.7

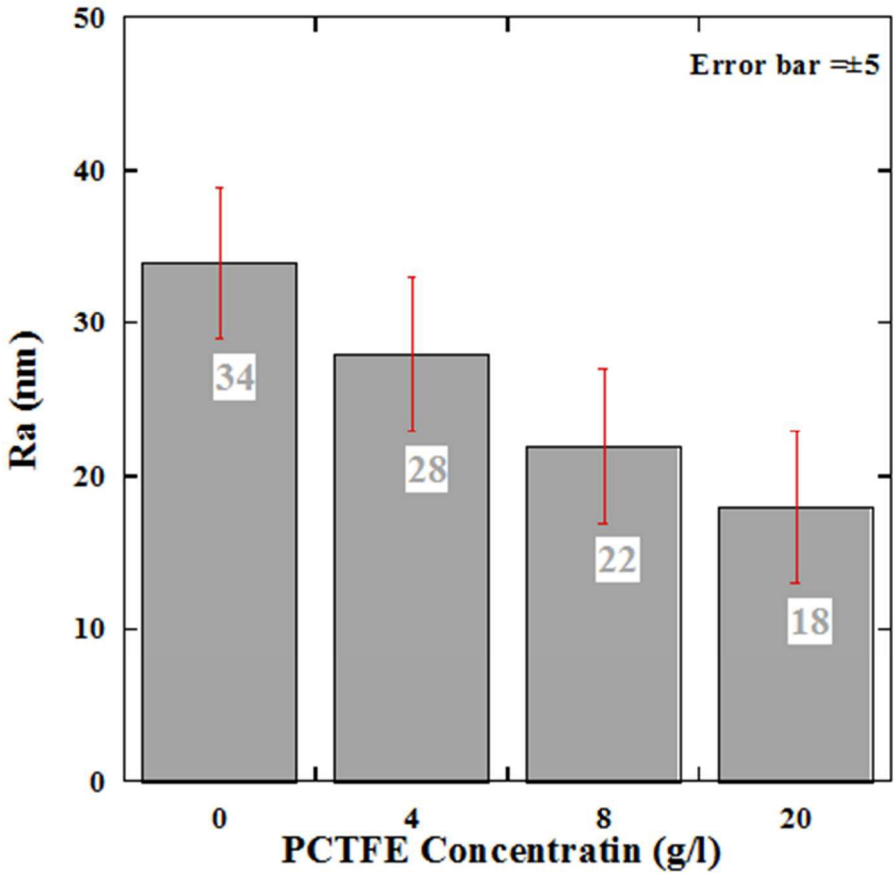

Fig.8

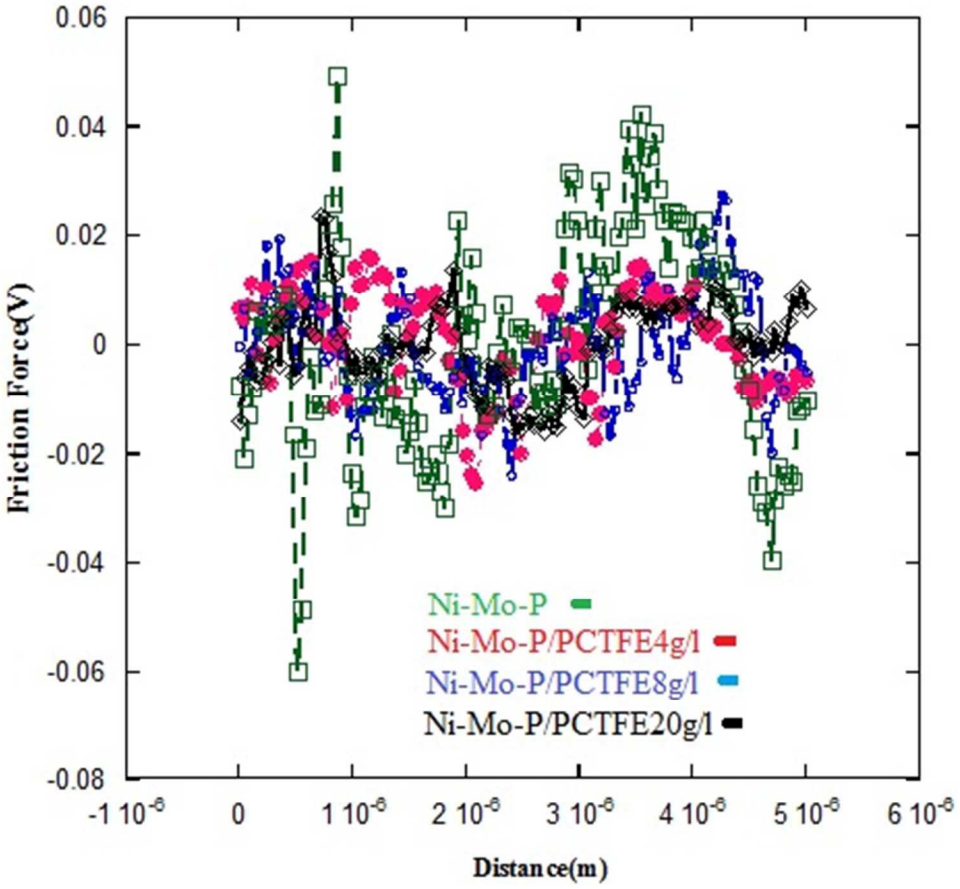

Fig.9

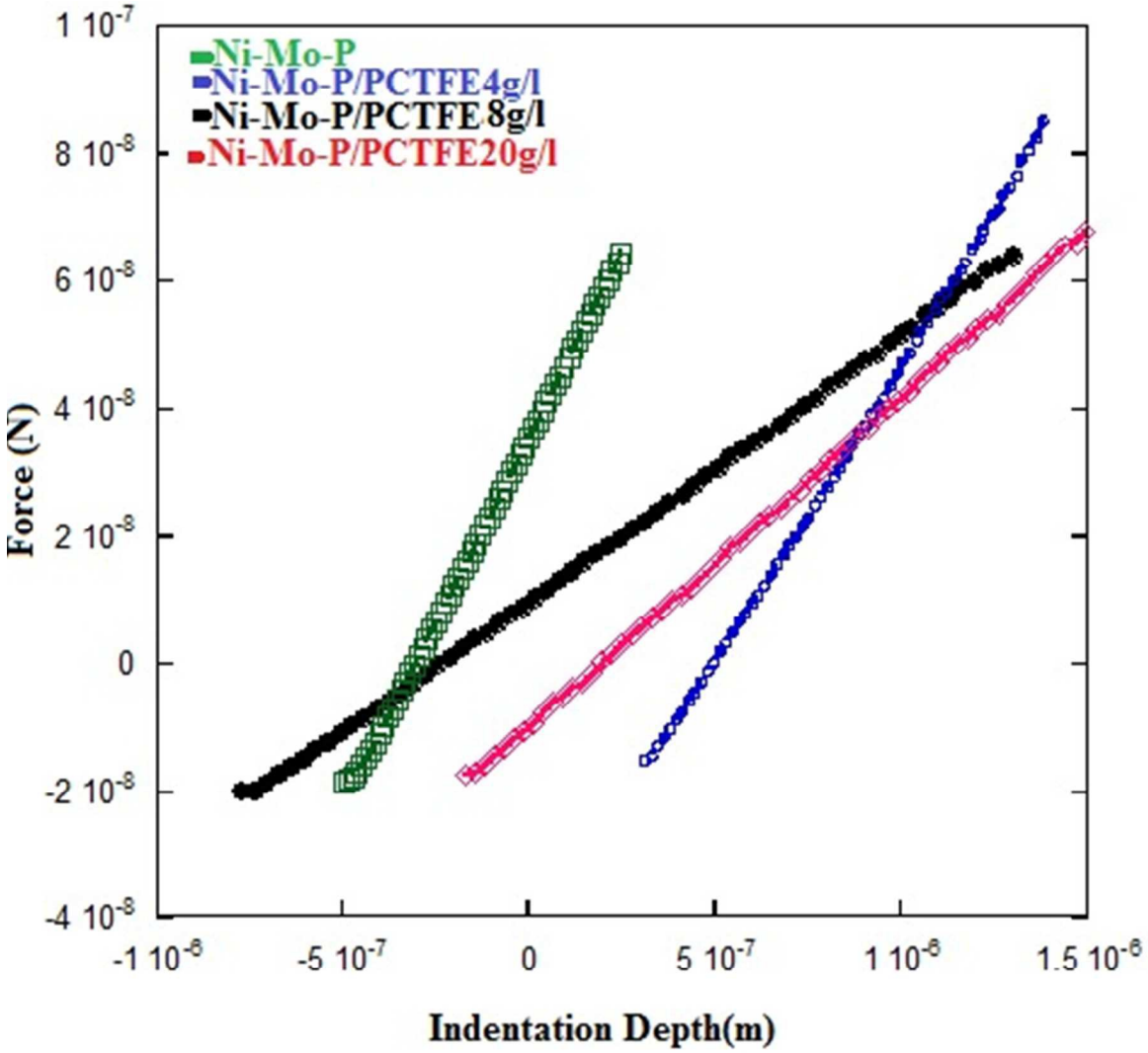

Fig.10

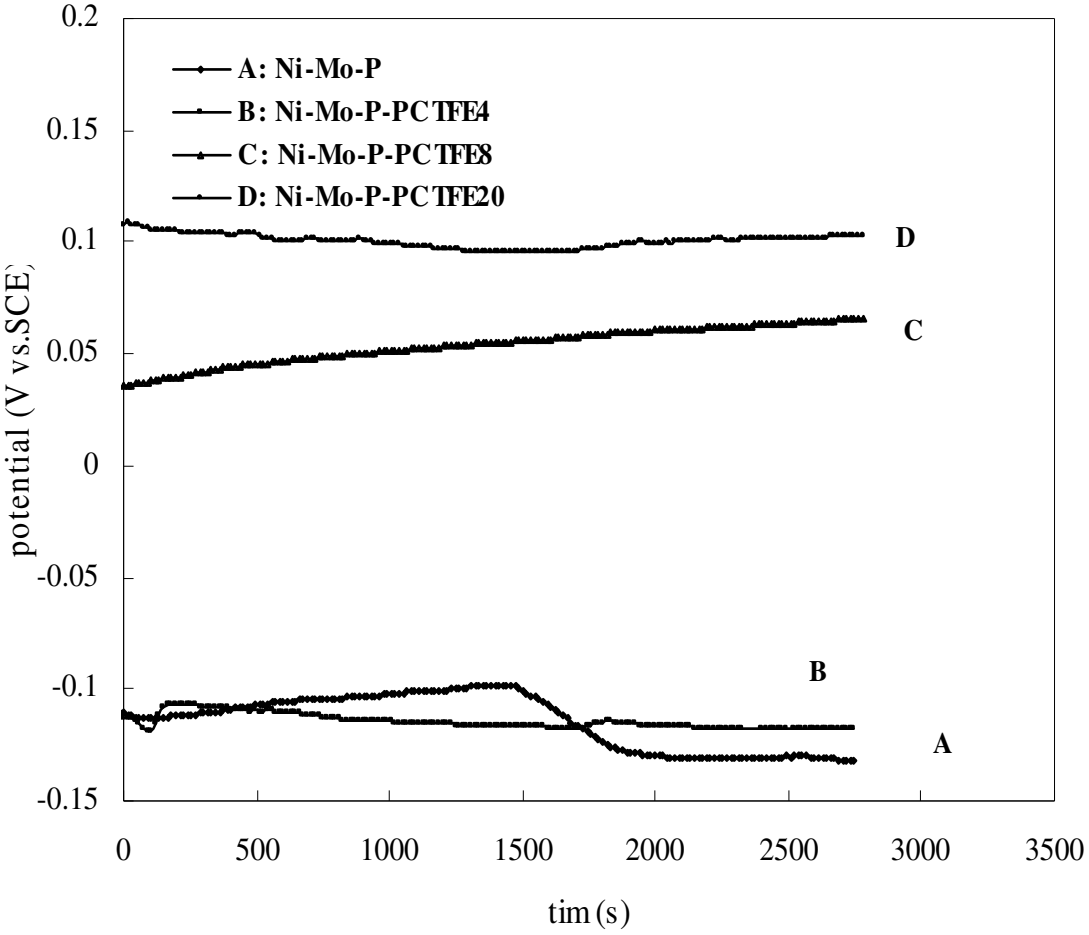

Fig.11

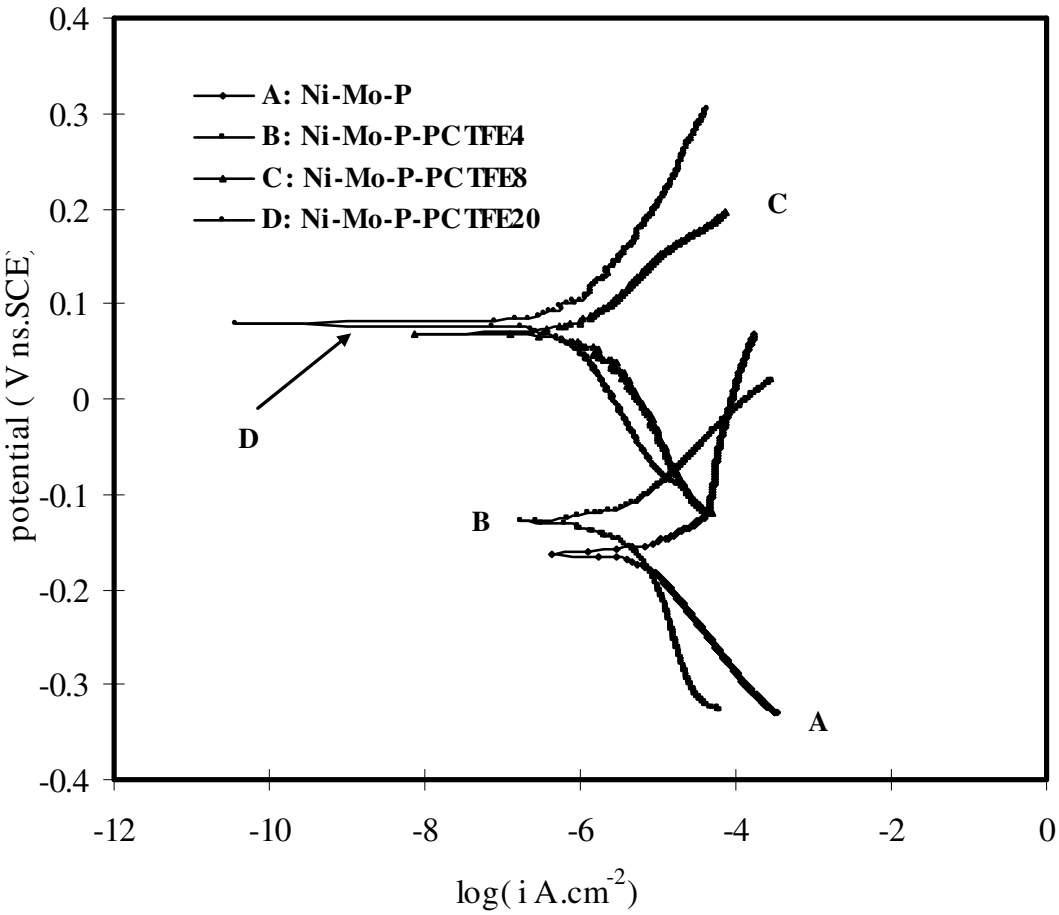

Fig.12

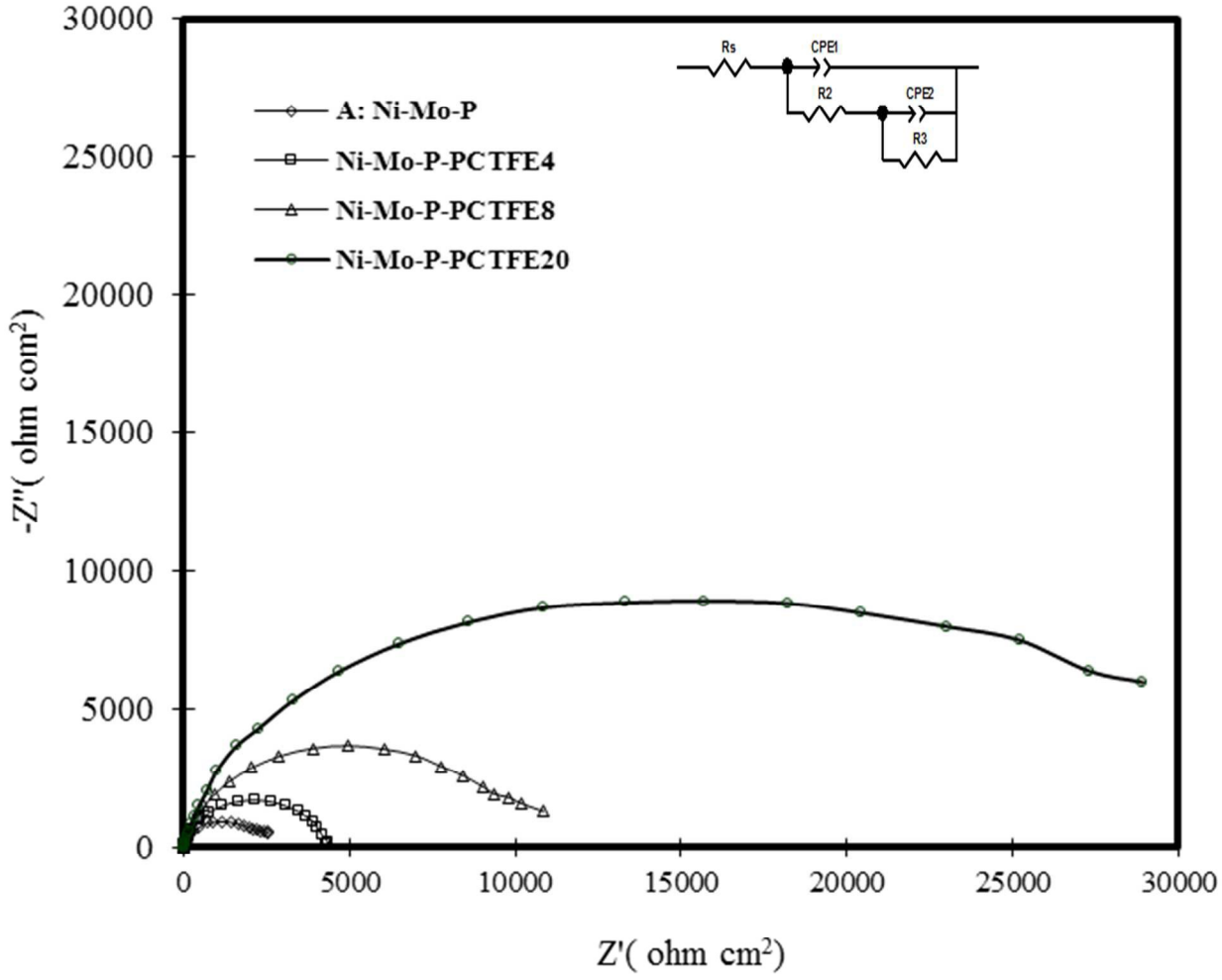

Fig.13

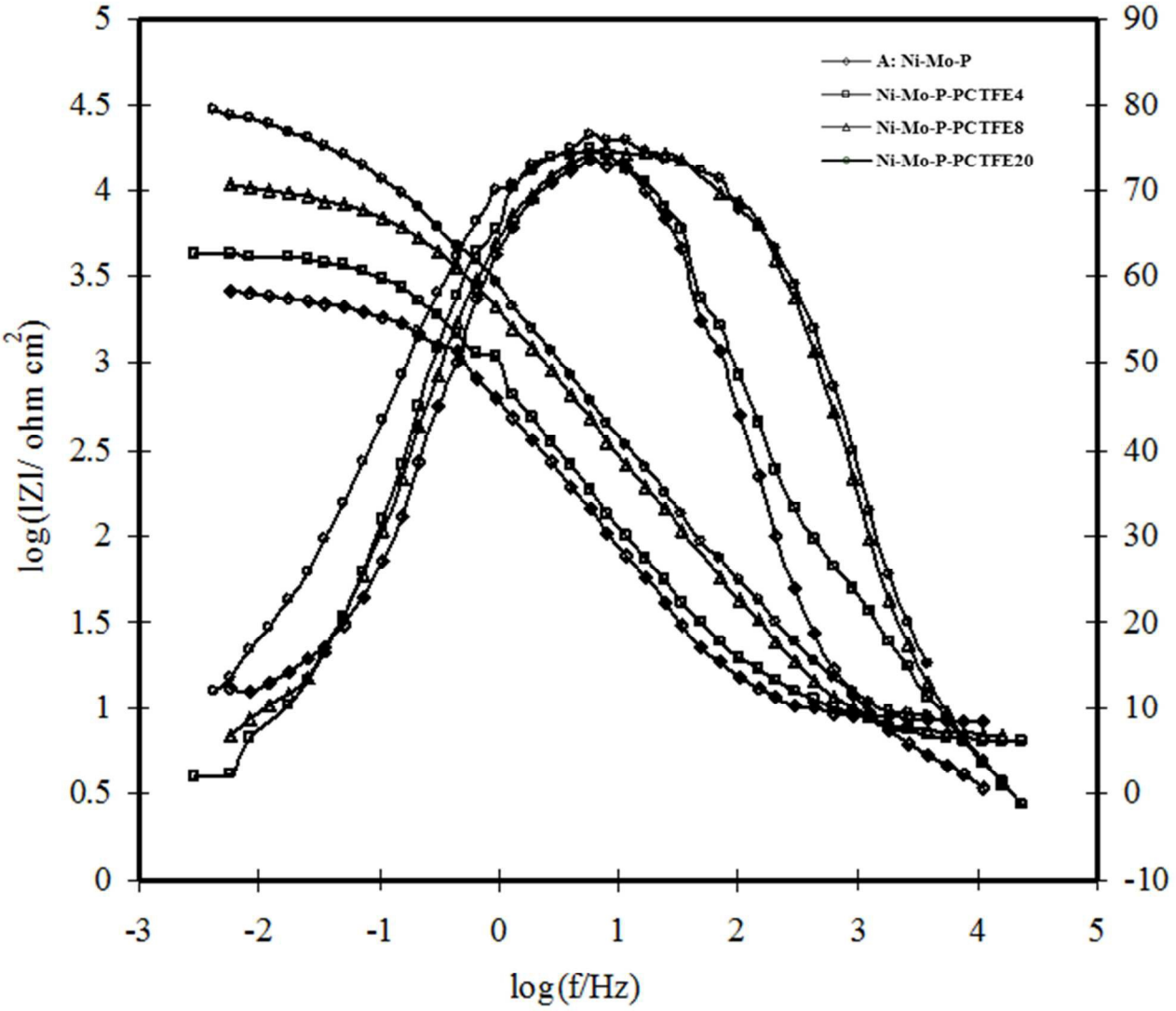

Fig.14

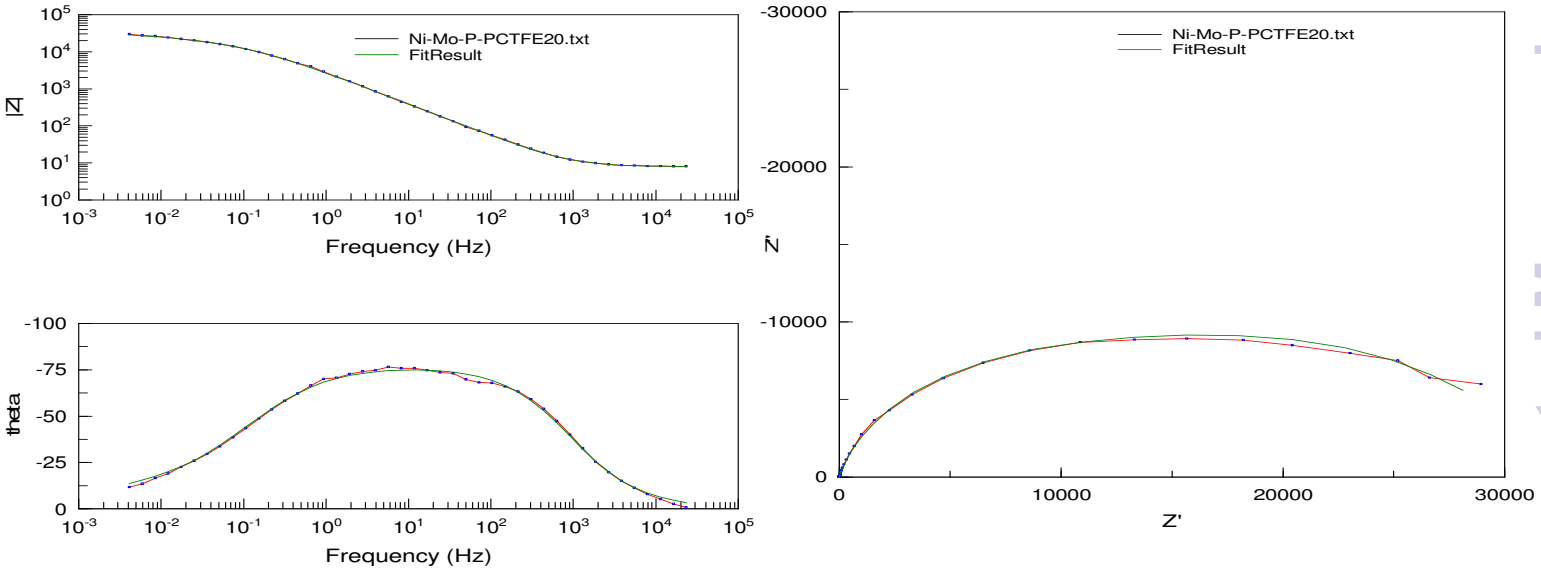

Fig.15